Available online at www.sciencedirect.com

SciVerse ScienceDirect

Ceramics International 39 (2013) 5733–5740

CERAMICS INTERNATIONAL

www.elsevier.com/locate/ceramint

Thermal and electrical properties of hot-pressed short pitch-based carbon fiber-reinforced ZrB_2–SiC matrix composites

Shuqi Guo*

Hybrid Materials Unit, National Institute for Materials Science, 1-2-1 Sengen, Tsukuba, Ibaraki 305-0047, Japan

Received 13 November 2012; accepted 30 December 2012
Available online 11 January 2013

Abstract

Short pitch-based carbon fiber-reinforced ZrB_2-20 vol% SiC matrix composites, with fiber volume fractions in the range of 0–50%, were manufactured by a hot-press process. Highly dense composite compacts were obtained at 2000 °C and 20 MPa for 60 min in Ar atmosphere. The microstructure of the resulting composites was characterized by scanning electron microscopy. The thermal and electrical properties of the composites were evaluated at room temperature. The effects of fiber volume fraction on these properties were assessed. The thermal and electrical conductivities decreased with increase of fiber volume fraction. The thermal conductivities of the composites were 48.3–104.7 W m^{-1} K^{-1}. The electrical conductivities of the composites were in the range 0.79×10^4–3.02×10^4 Ω^{-1} cm^{-1}.

Keywords: A. Hot pressing; B. Composites; C. Electrical conductivity; C. Thermal conductivity

1. Introduction

Hafnium and zirconium diborides belong to the refractory transition metal diborides from the fourth to sixth group of the periodic table. Most of theses diborides, typically ZrB_2 and HfB_2, have melting point above 3000 °C, high hardness, good wear resistance, excellent thermal conductivity, and high electrical conductivity, making them potential candidates for thermal protection structures for leading-edge parts on hypersonic re-entry space vehicles at over 1800 °C and/or for substrate on electrical device [1–3]. However, the use of ZrB_2 or HfB_2 ceramic materials, even fully densified, in thermomechanical structural applications is limited by their poor fracture resistance and damage tolerance.

One of the most promising solutions for improving fracture resistance and damage tolerance is to apply continuous ceramic fiber to monolithic ceramic for fabricating a fiber-reinforced ceramic matrix composite [4]. Recently, studies with short PAN- or pitch-based carbon fiber or/and SiC fiber-reinforced SiC-modified ZrB_2 or HfB_2 matrix composites showed the improved fracture toughness and damage tolerance as well as lowered density [5–8], as a result of crack bowing, and crack deflection or bridging and low density of fiber. In particular, the pitch-based carbon fiber-reinforced HfB_2-20 vol% SiC matrix composites showed higher strength at 1600 °C than at room temperature [8]. Hence, in addition to improvement of fracture toughness or/and damage tolerance due to incorporation of fiber, the high temperature strength of the composites was improved as well. Thus, compared to monolithic hafnium and zirconium diborides, the carbon or SiC fiber-reinforced ZrB_2 or HfB_2 matrix composites should be more suitable potential materials for the thermomechanical structural applications at high temperature. In particular, the pitch-based carbon fiber-reinforced ZrB_2-based matrix composites are considered as the most promising candidate materials for these applications, because the density of ZrB_2 is approximately half density of HfB_2 as well as the excellent thermal conductivity of pitch-based carbon fiber. However, the thermal and electrical properties of the composites and effects of fiber volume fraction are not well-known. The thermal and electrical properties are the important physical properties

*Tel.: +81 29 859 2223; fax: +81 29 859 2401.
E-mail address: GUO.Shuqi@nims.go.jp

0272-8842/$ - see front matter © 2013 Elsevier Ltd and Techna Group S.r.l. All rights reserved.
http://dx.doi.org/10.1016/j.ceramint.2012.12.091

for the ZrB_2-based ceramic composites when they are considered to use for refractory applications in thermo-mechanical structural applications or for substrate of electrical devices. Therefore, it is necessary for the carbon fiber-reinforced ZrB_2-based matrix composites to learn their thermal and electrical properties and the effects of fiber volume fraction.

In the present study, the short pitch-based carbon fiber-reinforced ZrB_2-20 vol% SiC matrix composites, with different fiber volume fractions between 10% and 50%, were manufactured by a hot-press process. The densification behavior of the composites was monitored by measuring the changes in sintering displacement with temperature along the pressure direction. The microstructures of the resulting composites were characterized by field emission scanning electron microscopy (FE-SEM). The thermal and electrical properties of the resulting composites were examined at room temperature by a nanoflash technique and a current–voltage method, respectively. Also, the effects of fiber volume fraction on the densification behavior, thermal and electrical properties of the composites were discussed.

2. Experimental procedure

The starting powders used in this study were: ZrB_2 (Grade O, Japan New Metals, Osaka), average particle size $\approx 2.12\,\mu m$, α-SiC (UF-15, H.C. Stack, Berlin, Germany), average particle size $\approx 0.5\,\mu m$, and pitch-based carbon fiber (XNG-90, Nippon Graphite Fiber Corporation, Tokyo), average fiber length ≈ 0.5 mm. The ZrB_2 and SiC powders (20% in volume) containing 2 wt% B_4C and 1 wt% C additives were mixed in ethanol using a silicon carbide media for 24 h. Subsequently, the short carbon fibers were added to the as-received ZrB_2-20 vol% SiC mixture slurry and the slurry were further mixed to a homogeneous mass using a planetary centrifugal mixer in ambient air for 3 min (ARE-310, Thinky Corporation, Tokyo). The resulting ZrB_2-20 vol% SiC slurry containing carbon fibers was then dried in oven. To examine effects of fiber volume fraction on the densification behavior, the thermal and electrical properties, six compositions of 0, 10, 20, 30, 40 and 50 vol% short pitch-based carbon fiber-reinforced ZrB_2-20 vol% SiC matrix composites (G_f/ZrB_2–SiC) were prepared in this study. Hereafter, the six compositions G_f/ZrB_2–SiC composites are denoted as ZSGF00, ZSGF10, ZSGF20, ZSGF30, ZSGF40, and ZSGF50 (Table 1), respectively.

The obtained powder mixtures were hot-pressed (NEW-HP5, Nissin Giken Co. Ltd., Saitama, Japan) in the graphite dies in tablets averaging 21 mm × 25 mm × 3.5 mm in size. The temperature of the sample was monitored by a two-color optical pyrometer through a hole opened in the die. To obtain highly dense samples, the powder compacts were heated to 2000 °C under a pressure of 20 MPa in a flowing Ar atmosphere with a heating rate of ~20 °C/min. After the hot press was held at 2000 °C for 60 min, the load was removed and the sample was cooled to 500 °C with ~15 °C/min, and the electric powder was then shut off.

After removing the surface of the hot-pressed compacts to avoid contamination from the graphite die, the bulk densities ρ, of the composites were measured by the Archimedes method with distilled water as the medium. The theoretical densities of the composites were calculated according to the rule of mixtures. Density values of 6.09 g/cm^3 for ZrB_2, 3.22 g/cm^3 for SiC, 2.52 g/cm^3 for B_4C, 1.8 g/cm^3 for C, and 2.12 g/cm^{3}for pitch-based carbon fiber are used in the calculation of theoretical density of the composites. The microstructure of the resulting composites was characterized by the FE-SEM. The grain sizes d, of ZrB_2 and SiC in the matrix were determined by measuring the average linear intercept length, d_m, of the grains in FE-SEM images of the composites, according to the relationship of $d = 1.56 d_m$ [9].

The thermal conductivity of the composites k_c, is determined from the thermal diffusivity α, heat capacity C_p, and density ρ, according to the following equation [10]:

$$K_c = \rho C_p \alpha \quad (1)$$

The thermal diffusivity was measured on a disk-shaped specimen with diameter of 10 mm and thickness of ~2 mm using the nanoflash technique (LFA447/2-4N, Nanoflash, NETZSCH-Geratebau GmbH, Postfach, Germany). Prior to the measurements, the samples were coated with a colloidal graphite spray to enhance the absorption of the

Table 1
The compositions, densities, and average grain diameter of the short pitch-based carbon fiber-reinforced ZrB_2-20 vol% SiC matrix composites consolidated by hot-pressing process.

Materials	Composition of matrix (wt%)				Fiber content V_f (vol%)	Bulk density (g cm^{-3})	Real density (g cm^{-3})	Relative density (%)	Average grain diameter, d (μm)	
	ZrB_2	SiC	B_4C	C					ZrB_2	SiC
ZSGF00	84.7	12.3	2	1	0	5.23	5.24	99.8	2.59 ± 1.01	1.31 ± 0.74
ZSGF10	84.7	12.3	2	1	10	4.91	4.93	99.6	2.55 ± 1.29	1.47 ± 0.86
ZSGF20	84.7	12.3	2	1	20	4.59	4.62	99.4	2.79 ± 1.31	1.65 ± 0.85
ZSGF30	84.7	12.3	2	1	30	4.29	4.31	99.5	2.82 ± 1.25	1.35 ± 0.59
ZSGF40	84.7	12.3	2	1	40	3.92	3.99	98.2	3.01 ± 1.32	1.36 ± 0.55
ZSGF50	84.7	12.3	2	1	50	3.61	3.68	98.1	2.37 ± 1.12	1.31 ± 0.71

Xenon light pulse energy and the emission of IR radiation to the temperature detector. The heat capacity was determined with alumina as the reference material.

Moreover, the electrical conductivity measurements of the composites were performed using the standard four-point probe method at room temperature to reduce the effects of contact resistance. A power supply (Model: 6220, Keithley, Cleveland, Ohio, USA) and digital multimeter (Model: 2182 Nanovoltmeter, Keithley) were used to measure the *I–V* characteristics of the samples. The detailed measurement procedures for the thermal and electrical conductivities had been reported elsewhere [11].

3. Results and discussion

3.1. Densification behavior

The typical shrinkage curves obtained during the hot pressing cycle for the six composition composites are shown in Fig. 1. It is found that the shrinkage behavior of the composites was linked to fiber volume fraction. The measurable shrinkage was initially observed at the temperature range between 1450 °C and 1780 °C for the six composition composites, depending on fiber volume fraction. For the ZrB_2-20 vol% SiC matrix without addition of carbon fiber, the noticeable shrinkage initially occurred at approximately 1450 °C. For comparison, the onset temperature of densification of the composites was determined to be ~1460 °C for ZSGF10, ~1470 °C for ZSGF20, ~1540 °C for ZSGF30, ~1560 °C for ZSGF40, and ~1780 °C for ZSGF50. Although the onset temperature shifted a higher temperature with increase of fiber volume fraction, the significantly raised temperature was observed only for a fiber volume fraction equal to or greater than 30%. In other words, the onset temperature of densification is almost the same for the composites which fiber volume fraction is equal to or less than 20%, regardless of fiber volume fraction. However, for 50 vol% fibers-containing composite (ZSGF50) the onset temperature of densification was markedly raised and it was ~330 °C higher than that of the matrix (ZSGF00). The increase in the onset temperature of densification due to the presence of the fiber showed that the densifying mechanism of the ZrB_2–SiC matrix powder, such as grain boundary diffusion and grain boundary migration, was inhibited during the heating. Hence, the activated densification of the matrix was shifted to a higher temperature, as a result of the presence of fiber.

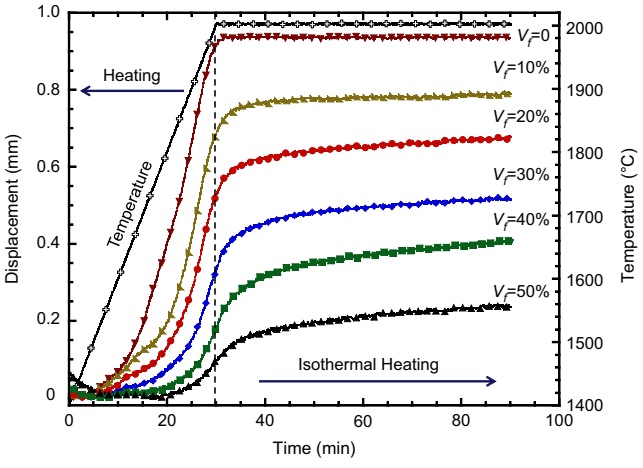

Fig. 1. Typical shrinking curves obtained during the hot-pressing cycle for the short pitch-based carbon fiber-reinforced ZrB_2-20 vol% SiC matrix composites.

During the subsequent densification followed the activated temperature, a rapid shrinkage region was observed in the displacement–time curves with further increasing temperature for all the composites (Fig. 1). The shrinkage rate depended on the amount of fiber and it decreased with increase of fiber volume fraction. This indicated that the presence of fiber hindered the densification progress of the matrix. In addition, the observed rapid shrinkage region became narrow with the fiber volume fraction. This suggests that the resistance to densification due to the presence of fiber increased with amount of fiber. For the ZrB_2-20 vol% SiC matrix (ZSGF00), the rapid shrinkage almost ended when the temperature approached to 2000 °C. For the other compositions, the rapid shrinkage ended after the holding time of ~5 min at 2000 °C.

On the other hand, for ZSGF00 composition the shrinkage was not observed during the isothermal heating. This suggests that the densification was completed during the heating. Relative density exceeding 99% was obtained for ZSGF00 composition at 2000 °C and 20 MPa for 60 min (Table 1). An early study in the hot-pressed ZrB_2-20 vol% SiC composition showed that the densification required 1900 °C at 20 MPa for 60 min. For the other five compositions, the densification was not completed during the heating and the densification carried out continuously during the subsequent isothermal heating. For ZSGF10, the noticeable shrinkage was observed only within ~10 min followed the isothermal heating, and then a plateau was observed in the curve. Hence, for ZSGF10 the main part of densification occurred during the heating. For a composite with the fiber volume fraction equal to or greater than 20%, however, the shrinkage proceeded during the isothermal heating until the end of sintering, absence of the plateau in the curve. Relative density exceeding 98% was obtained for these compositions composites at 2000 °C and 20 MPa for 60 min (Table 1). This indicated that highly-dense composite compacts could be manufactured, by using the hot press process.

3.2. Microstructure characterization

To characterize the dispersion condition of fibers in the resulting composites, the five compostions samples were observed at low-magnification under FE-SEM, typical examples of which are shown in Fig. 2. It is found that the short carbon fibers were randomly and uniformly dispersed in the matrix without the aggregation of fibers for all the composition composites, independent on fiber

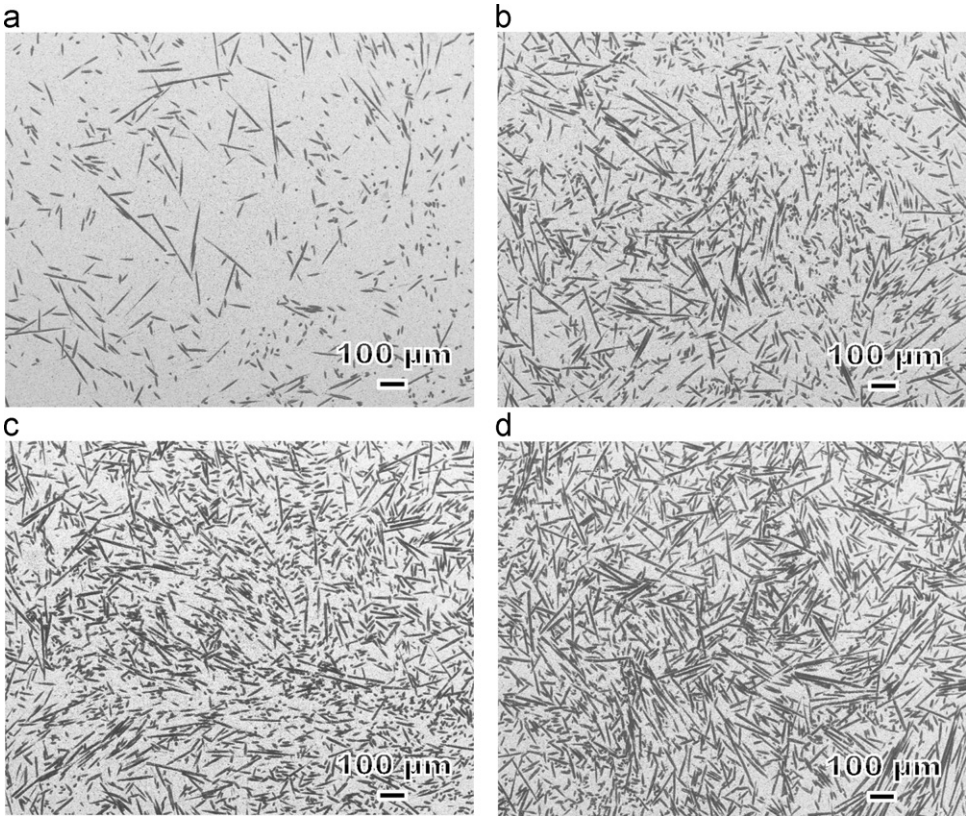

Fig. 2. Typical examples of FE-SEM micrographs of the microstructures for the composites: (a) ZSGF10, (b)ZSGF30, (c) ZSGF40, and (d) ZSGF50.

volume fraction. The absence of the fiber clumps suggests that the short fibers were homogeneously dispersed in the matrix slurry after mixing. This indicated that the mixing method used in this study is very effective for homogeneously dispersing short fibers in ceramic slurry although the mixing time was very short (only 3 min). This short mixing time may reduce the damage of fibers due to mixing. In addition, the large macro-defects such as pores and cracks were not observed, showing highly dense composites, which agrees with the high densities measured in the resulting composites (Table 1).

Under high-magnification (Fig. 3), although no pore was observed for a fiber volume fraction equal to or less than 30% (Fig. 3(a)), several small pores were observed at the fiber/matrix interface or at multi-fibers junctions for a composite containing equal to or greater than 40 vol% fibers (indicated by arrows in Fig. 3(b)). In addition, it is found that the matrix showed a homogeneous and fine grain microstructure and it consisted of the equiaxed ZrB_2 (brighter contrast) and SiC (dark contrast) grains (Fig. 3(c) and (d)). The grain sizes of ZrB_2 and SiC measured in six compositions composites were summarized in Table 1. For ZrB_2 phase, the grain size increases with increase of fiber volume fraction, with particles size ranging from 2.55 to 3.01 μm. Apparently, the average grain diameter of ZrB_2 was larger than that of starting powder (2.12 μm), as a result of grain growth during the sintering. Presumably, the coarseness of ZrB_2 grains due to addition of fiber is a result of the hindered effect of fiber from breaking apart the agglomeration of ZrB_2 particles during the mixing process. One exception was nearly the same grain size of ZrB_2 for both the ZSGF00 and ZSGF50 composites, regardless of the presence of fiber. This suggests that the hindered effect of fiber disappeared when the fiber volume fraction is equal to 50%. For SiC phase, on the other hand, the grain size increased as the fiber volume fraction increased from 0% to 30%, then the grain size retained almost the constant and its size was similar to that of ZSGF00, regardless of the amount of fibers. The SiC grains had a particles size ranging from 1.31 to 1.65 μm, which is larger than that of the starting powder (~0.5 μm). It is evident that the addition of fiber hindered from breaking apart the agglomeration of SiC particles during the mixing process. As a result, the clusters of SiC particles were fused together during hot pressing to form larger SiC particles. However, the hindered effect of fiber was observed only for a fiber volume fraction equal to or less than 30%.

Fig. 4 showed typical examples of FE-SEM micrographs near the boundary between the fiber and the matrix for a longitudinal fiber and transverse fiber in the composites. In the cross-section (Fig. 4(a)), the surface of fiber exhibits an inherent saw-toothed front shape. In addition, several porosities were observed within the fiber. In the plan-section (Fig. 4(b)), the fibers appear to be uniform in structure. This suggests that there is little difference in

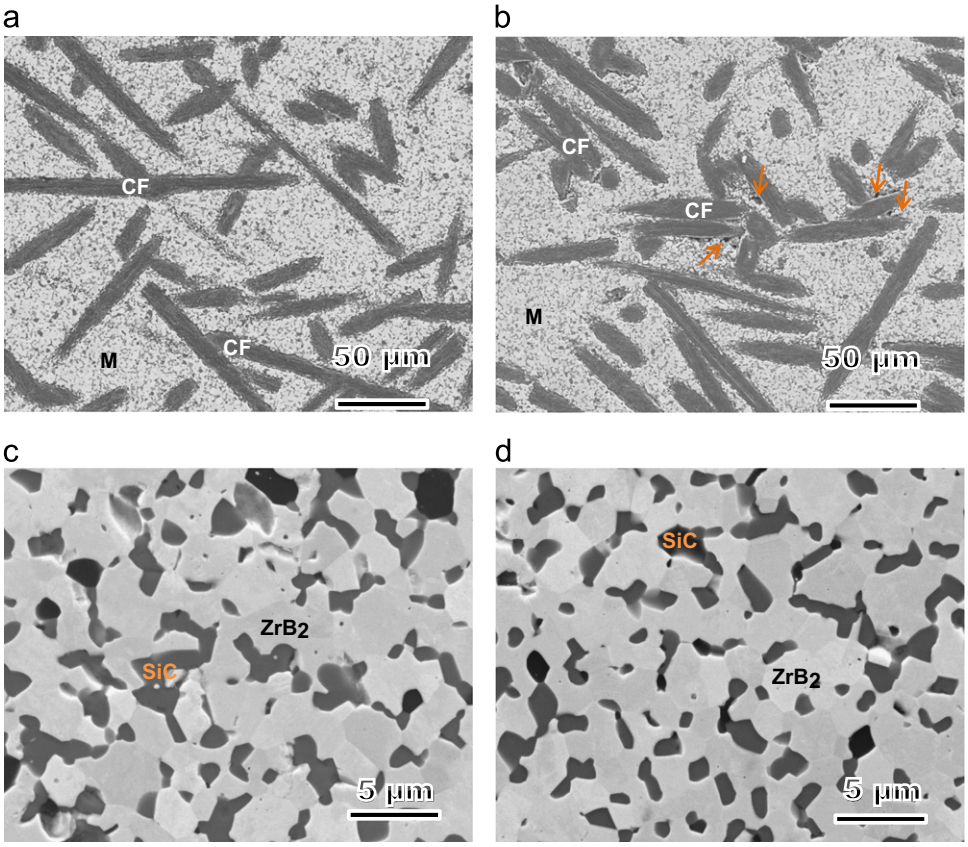

Fig. 3. Typical examples of high-magnification FE-SEM micrographs of the microstructures for the composites: (a) ZSGF30, (b)ZSGF40, (c) ZSGF10, and (d) ZSGF50, (CF: carbon fiber, M: matrix).

microstructure across the fiber section. In addition, it is found that the fiber consisted of a lot of thin sheets and the gaps were presented between the sheets. Naito et al., [12] had previously reported that the pitch-based fibers have a sheet-like microstructure and the crystallite sheets were well-defined and less curved. Additionally, there are gaps between the crystallite sheets, which led to pull out of the sheets at failure. On the other hand, an earlier study in a PAN-based carbon fiber-reinforced ZrB_2–SiC composite consolidated by hot-press at 2000 °C showed the presence of the interfacial reaction layer between the fiber and matrix [5]. Although similar interfacial reaction should be expected for the pitch-based carbon fiber reinforced-ZrB_2-20 vol% SiC matrix composites investigated in this study, a noticeable interface reaction layer was not observed between the fiber and the matrix in the both sections (Fig. 4), and further detailed investigation is needed.

3.3. Thermal properties

In Fig. 5, the heat capacity and thermal diffusivity as a function of fiber volume fraction for the composites are presented. From this figure, it is found that the heat capacity was almost constant for the composites, regardless of fiber volume fraction. For comparison, the thermal diffusivity linearly decreased with increasing fiber volume fraction. This suggests that the thermal conductivity of the composites is mostly dominated by the thermal diffusivity in the composites. The lowered thermal diffusivity due to addition of carbon fiber indicated that the added fibers led to increase in resistance to the heat flow in the composites through the components and their interfaces, and this thermal resistance was enhanced with increase of fiber volume fraction. The thermal conductivity of the composites as a function of fiber volume fraction is shown in Fig. 6. The composites showed a good thermal conductor, with thermal conductivities in the range of 48–105 W/m K. The thermal conductivity of the composites monotonously decreased with increase of fiber volume fraction. The dependency of thermal conductivity on fiber volume fraction is similar to that of thermal diffusivity. This similar dependency of fiber volume fraction indicated that the thermal conductivity of the composites is dominated by the heat flow in the composites.

It is known that the thermal conductivity of the composites depended on the thermal conductivity of the components and the interfacial thermal resistance between the fiber and the matrix. Although the pitch-based carbon fiber used in this study has very high thermal conductivity (500 W/m K), compared to the ZrB_2-20 vol% SiC matrix (105 W/m K), the thermal conductivity of the composites

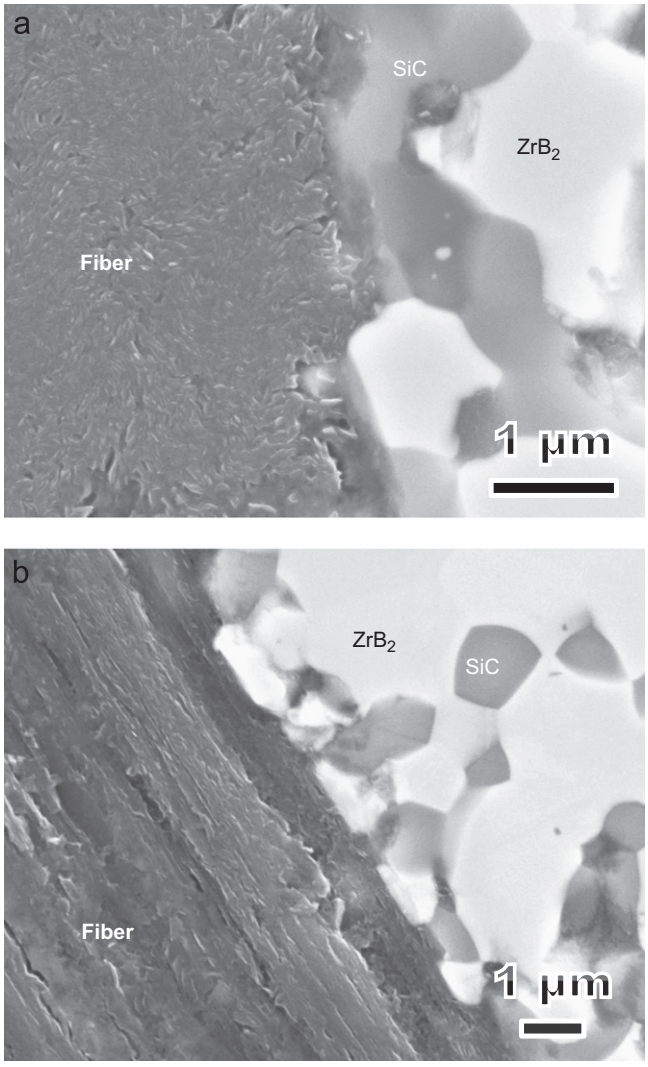

Fig. 4. Typical examples of FE-SEM micrographs of the interface between the fiber and the matrix for the composites: (a) cross-section, ZSGF40, and (b) plan-section, ZSGF10.

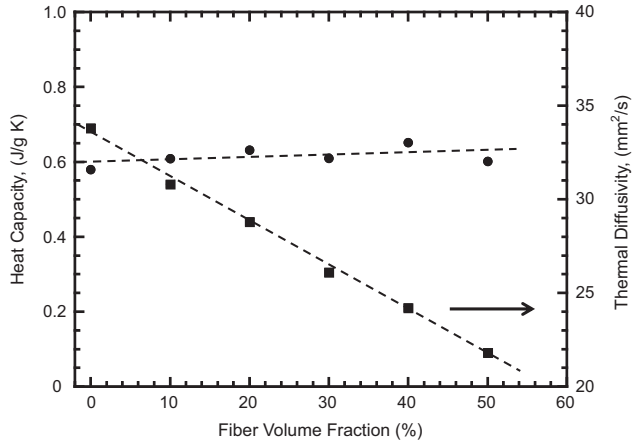

Fig. 5. Plots of the heat capacity and thermal diffusivity of the composites as a function of fiber volume fraction.

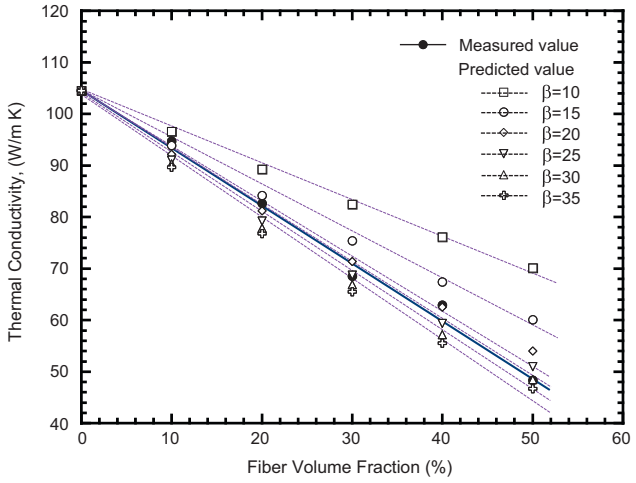

Fig. 6. Plots of the thermal conductivity of the composites as a function of fiber volume fraction.

decreased with increasing fiber volume fraction. As a result, the decrease in thermal conductivity due to addition of fiber is believed to be attributed to the interfacial thermal resistance between the fiber and the matrix [13]. It is evident that the interfacial thermal resistance increased with fiber volume fraction, therefore decreased thermal conductivity. An early theoretical study [14] in a composite-containing circular cylindrical dispersions showed that thermal conductivity of the composite was predicted by a simple equation. Assuming the interactions between the local temperature fields of neighboring dispersions are negligible, the thermal conductivity of the composites, k_c is given by [14]

$$K_c = K_m \frac{(\gamma-\beta-1)V_f+(1+\gamma+\beta)}{(1+\gamma-\beta)V_f+(1+\gamma+\beta)} \quad (2)$$

where β is the nondimensional parameter, γ ($\gamma=k_f/k_m$) is the ratio of thermal conductivity of fiber to thermal conductivity of matrix, and V_f is the fiber volume fraction. The β is given by

$$\beta = \frac{K_f}{R_f h_i} \quad (3)$$

where k_f is the thermal conductivity of the fiber, R_f ($=5$ μm) is the radius of fiber, and h_i is the interfacial conductance between the fiber and the matrix, ranging from 0 to ∞. For $h_i=0$ (i.e. $\beta=\infty$), no heat can flow across the interface between the fiber and the matrix into the fibers, which then can not contribute to the transfer of heat, irrespective of the absolute value of k_f. For $h_i=\infty$ (i.e. $\beta=0$), heat can completely across the interface between the fiber and the matrix into the fibers, without the interfacial thermal barrier resistance. With $k_m=105$ W/m K (Fig. 6) and $k_f=500$ W/m K, and taking β value ranging from 10 to 35, the thermal conductivities of the composites are calculated by Eq. (2), whose results are shown in Fig. 6. It is found that the predicted thermal

conductivities of the composites roughly agree with the experimental measurements when β value ranges from 20 to 30. In particular, for $\beta=25$ the predicted values are the most close to the experimental data. This agreement indicated that the dependency of the fiber volume fraction for the thermal conductivity of the composites is mainly dominated by the interface thermal transport between the fiber and the matrix. Thus, it is believed that the decreased thermal conductivity due to addition of fiber could be due to high interface thermal resistance across the fiber/matrix interface for the composites investigated in this study.

3.4. Electrical properties

In Fig. 7, the electrical resistivity of the omposites as a function of fiber volume fraction is presented. The electrical resistivity of the composites monotonously increased with increasing fiber volume fraction. An early systemic study on effect of amount of SiC on the electrical resistivity in the ZrB_2–SiC composites showed that the electrical resistivity sharply increased with SiC content over 70 vol% [15], i.e., the presence of an electrical percolation threshold. However, the electrical percolation threshold was not observed in the composites investigated in this study. The studied composites showed a good electrical conductor, with the electrical resistivities in the range of $3.32\times10^{-5}-12.66\times10^{-5}\Omega$ cm. The corresponding electrical conductivities are in the range $0.79\times10^{4}-3.02\times10^{4}\Omega^{-1}\,cm^{-1}$. The increase in electrical resistivity due to the addition of fiber is a result of the high electrical resistivity of the fiber, because the electrical resistivity of the fiber ($30.2\times10^{-5}\Omega$ cm) is much greater than that of ZrB_2-20 vol% SiC matrix ($3.32\times10^{-5}\Omega$ cm). The presence of fiber produces a higher resistance to electron mobility in the composites and the resistance increases with increase of fiber volume fraction, therefore high electrical resistivity. The electrical resistivity in the composite which consists of a continuous matrix and dispersed phase, δ_c, is given by [16]

$$\delta_c=\delta_m\frac{1+ABV_f}{1-B\varphi V_f} \tag{4}$$

$$B=\frac{\delta_f/\delta_m-1}{\delta_f/\delta_m+A} \tag{5}$$

$$\varphi\approx1+\left(\frac{1-\phi}{\phi^2}\right)V_f \tag{6}$$

Where δ_m and δ_f are the electrical resistivity of the matrix and the fiber, respectively, A is a constant for any given composite and it depends primarily on the shape of the dispersed phase and how it oriented with respect to the direction of flow of electrical currents, and ϕ is the maximum packing fraction of the dispersed phase. In addition, Eqs. (4)–(6) include an infinite number of mixture laws. When $A\to\infty$ and $\phi=1$, the Eqs. (4)–(6) are in the original Halpin–Tsai equation, and they become the rule of mixture as following:

$$\delta_c=\delta_m(1-V_f)\delta_f V_f \tag{7}$$

when $A\to0$, the equations become the inverse rule of mixtures,

$$\frac{1}{\delta_c}=\frac{1-V_f}{\delta_m}+\frac{V_f}{\delta_f} \tag{8}$$

Obviously, Eqs. (7) and (8) are generally named the rule of mixtures and they are used to predict electrical resistivity in parallel to fiber and transverse to fiber for a continuous fiber-reinforced matrix composite. Intermediate values of A give mixture rules which are between these upper and lower bounds.

In the studied short-fiber-reinforced ceramic matrix composites with three dimensional random (Fig. 2), the constants A and ϕ are taken approximately 1 and 0.52 [16], respectively. With $\delta_m=3.32\times10^{-5}\,\Omega$ cm and $\delta_f=30.2\times10^{-5}\,\Omega$ cm, the electrical resistivity of the composites as a function of fiber volume fraction was predicted by Eqs. (4)–(6), as shown in Fig. 7. It is found that the predicted electrical resistivity well-agreed with the experimental measurements in the composites investigated in the present study. One exception is the high predicted electrical resistivity value for the case of 50 vol% fibers which is approximately equal to the maximum packing fraction of the fibers ($\phi=0.5$), i.e., $\phi\approx V_f$. An early theoretical study in the electrical resistivity in two-phase systems [16] demonstrated that the predicted values by Eqs. (4)–(6) are somewhat too high when $\phi=V_f$ if the discontinuous dispersed phase is the more resistant of the two phases. Presumably, the discrepancy at $\phi\approx V_f$ is that the φV_f approaches to 1.0 which is considered as a reduced concentration when the maximum packing fraction of the fibers is equal to the fiber volume fraction for the composites ($\phi=V_f$) rather than at $V_f=1$. This suggests that the interfacial effect between the fiber and the matrix needs be considered in the prediction of the electrical resistivity of the composite when the fiber volume fraction approaches to the maximum packing fraction of the fiber in the composites.

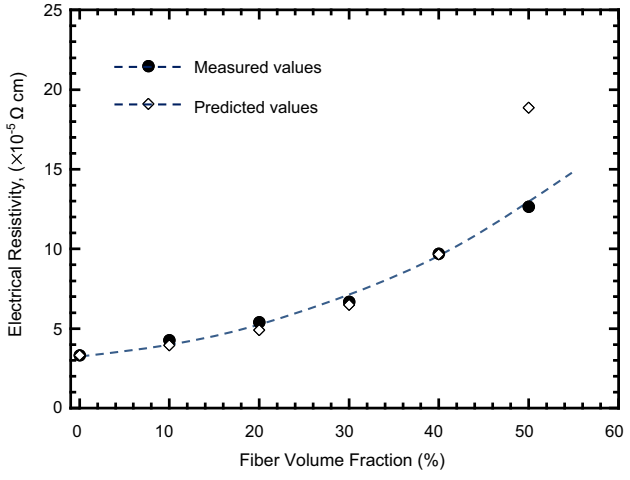

Fig. 7. Plots of the electrical resistivity of the composites as a function of fiber volume fraction.

4. Conclusions

In summaries, highly dense short pitch-based carbon fiber-reinforced ZrB_2-20 vol% SiC matrix composites, with fiber volume fraction ranging from 0% to 50%, were prepared by hot-press process at 2000 °C and 20 MPa for 60 min. The composite microstructure exhibited that the short fibers were randomly and uniformly embedded in the homogeneous equiaxed ZrB_2 and SiC grains matrix microstructure. The thermal conductivity of the composite decreased with increase of fiber volume fraction, with the conductive values range 48.3–104.7 $W\,m^{-1}\,K^{-1}$. The decrease due to addition of fiber is attributed to the interfacial thermal barrier resistance between the fiber and the matrix. In addition, the electrical resistivity of the composites was in the range 3.32×10^{-5}–$12.66 \times 10^{-5}\,\Omega\,cm$, and the electrical resistivity increased with increase of fiber volume fraction.

Acknowledgments

Author would to give special thanks to Dr. T. Nishimura, National Institute for Materials Science (NIMS), for his assistances with thermal conductivity measurements.

References

[1] K. Upadhya, J.-M. Yang, W.P. Hoffmann, Materials for ultrahigh temperature structural applications, American Ceramic Society Bulletin 76 (1997) 51–56.
[2] E. Wuchina, E. Opila, M. Opeka, W. Fahrenholtz, I. Talmy, UHTCs: Ultra-high temperature ceramic materials for extreme environment applications, Interface 16 (2007) 30–36.
[3] A. Paul, D.D. Jayaseelan, S. Venugopal, E. Zapata-Solvas, J. Binner, B. Vaidhyanathan, A. Heaton, P. Brown, W.E. Lee, UHTS composites for hypersonic applications, American Ceramic Society Bulletin 91 (2012) 22–29.
[4] W.C. Tu, F.E. Lange, A.G. Evans, Concept for a damage-tolerant ceramic composite with a strong interfaces, Journal of the American Ceramic Society 79 (1996) 417–424.
[5] F. Yang, X. Zhang, J. Han, S. Du, Processing and mechanical properties of short carbon fibers toughened zirconium diboride-based ceramics, Materials and Design 29 (2008) 1817–1820.
[6] F. Yang, X. Zhang, J. Han, S. Du, Characterization of hot-pressed short carbon fiber reinforced ZrB_2–SiC ultra-high temperature ceramic composites, Journal of Alloys and Compounds 472 (2009) 395–399.
[7] L. Silvestroni, D. Sciti, C. Melandri, S. Guicciardi, Toughened ZrB_2-based ceramics through SiC whisker or SiC chopped fibers reinforced additions, Journal of the European Ceramic Society 30 (2010) 2155–2164.
[8] S.Q. Guo, K. Naito, Y. Kagawa, Mechanical and physical behaviors of short pitch-based carbon fiber-reinforced HfB_2–SiC matrix composites, Ceramics International 39 (2013) 1567–1574.
[9] M.I. Mendelson, Average grain size in polycrystalline ceramics, Journal of the American Ceramic Society 52 (1969) 443–446.
[10] W.J. Parker, W.J. Jenkins, C.P. Butler, G.L. Abbott, Flash method of determining thermal diffusivity, heat capacity and thermal conductivity, Journal of Applied Physics 32 (1961) 1679–1684.
[11] S.Q. Guo, T. Nishimura, Y. Kagawa, H. Tanaka, Thermal and electric properties in hot-pressed ZrB_2–$MoSi_2$–SiC composites, Journal of the American Ceramic Society 90 (2007) 2255–2258.
[12] K. Naito, Y. Tanaka, J.-M. Yang, Y. Kagawa, Tensile properties of ultrahigh strength PAN-based, ultrahigh modulus pitch-based and high ductility pitch-based carbon fibers, Carbon 46 (2008) 189–195.
[13] R. Sivakumar, S.Q. Guo, T. Nishimura, Y. Kagawa, Thermal conductivity in multi-wall carbon nanotube-silica-based nanocomposites, Scripta Materialia 56 (2007) 265–268.
[14] D.P.H. Hasselman, L.F. Johnson, Effective thermal conductivity of composites with interfacial thermal barrier resistance, Journal of Composite Materials 21 (1987) 508–515.
[15] R. Jimbou, K. Takahashi, Y. Matsushita, T. Kosugi, SiC–ZrB_2 electroconductive ceramic composite, Advanced Ceramic Materials 1 (1986) 341–345.
[16] L.E. Nieisen, The thermal and electrical conductivity of two-phase systems, Industrial and Engineering Chemistry Fundamentals 13 (1974) 17–20.